Knockdown of MSI1 inhibits the proliferation of human oral squamous cell carcinoma by inactivating STAT3 signaling

CHEN-FEI WANG[1,2], HONG-CHUANG ZHANG[1,3], XIN-MEI FENG[2], XIAO-MENG SONG[1,3] and YU-NONG WU[1,3]

[1]Jiangsu Key Laboratory of Oral Diseases, Nanjing Medical University, Nanjing, Jiangsu 210000;
[2]Department of Oral and Maxillofacial Surgery, Affiliated Hospital of Nantong University, Nantong, Jiangsu 216000;
[3]Department of Oral and Maxillofacial Surgery, Affiliated Hospital of Stomatology,
Nanjing Medical University, Nanjing, Jiangsu 210000, P.R. China

Abstract. Musashi RNA-binding protein 1 (MSI1) is highly expressed in several types of cancer; however, its role in oral squamous cell carcinoma (OSCC) remains unknown. The purpose of this study was to investigate the probable mechanism underlying the involvement of MSI1 in OSCC. The results demonstrated that MSI1 was upregulated in OSCC tissues, but not in adjacent healthy tissues. MSI1 silencing resulted in decreased cell proliferative, invasive and migrative capacity. In addition, MSI1 silencing led to cell cycle arrest at the S phase, downregulation of c-Myc and cyclin D1, and upregulation of p21 and p27 levels. Additional studies demonstrated that MSI1 suppression inhibited the activation of signal transducer and activator of transcription 3 (STAT3) signaling. Accordingly, the findings of the present study suggested that MSI1 silencing can suppress OSCC cell proliferation and progression, in part by inhibiting the activation of the c-Myc/STAT3 pathway.

Introduction

Oral squamous cell carcinoma (OSCC) is one of the most common head and neck malignancies (1), as well as one of the most common epithelial cancers worldwide (2). A variety of etiological factors, such as smoking and alcohol consumption, have been associated with the development of OSCC (3). Despite improvements and innovations in diagnosis and treatment, the overall 5-year survival rate of OSCC patients is <50% (4,5). The standard treatment options for OSCC are surgery, chemotherapy and radiotherapy, with the latter

considered as an efficient adjuvant treatment for some cases of OSCC.

Previous studies have demonstrated that tumor stem cells are responsible for tumor metastasis (6,7), and an increasing number of stem cell-related genes have been proven to be involved in tumorigenesis (8,9). MSI1 is a RNA-binding protein of the Musashi family that has been found to be associated with certain cancers, including glioma (10), cervical cancer (11), gastric cancer (12) and lung cancer (13,14). In addition, MSI1 appears to be a prognostic marker for esophageal SCC (15) and glioma (16). Furthermore, MSI1 has been found to activate the AKT (14) and Notch (17,18) signaling pathways in certain types of cancer; however, its role in OSCC remains unclear. The aim of the present study was to investigate the role of MSI1 in OSCC progression and elucidate the underlying mechanism, as well as determine whether MSI1 acts as an oncogene in OSCC.

Materials and methods

Tissue collection. The study protocol was approved by the Ethics Committee of the Affiliated Hospital of Nantong University (Nantong, China). A total of 20 pairs of OSCC tissue and adjacent healthy tissue samples were collected between March 2015 and April 2017 at the Affiliated Hospital of Nantong University. All the patients provided written informed consent for their tissues to be used for research purposes. None of the patients had received radiation therapy prior to surgical resection. The collected tissues were immediately snap-frozen in liquid nitrogen for later use.

Cell culture, vector construction and cell transfection. The OSCC cell lines HSC-3, Ca9-22, SAS and OSC-19 were purchased from American Type Culture Collection. The HSC-3, SAS and OSC-19 cell lines were cultured in Dulbecco's modified Eagle's medium (DMEM; Sigma-Aldrich; Merck KGaA) supplemented with 10% fetal bovine serum (FBS; HyClone; GE Healthcare Life Sciences), and Ca9-22 cells were maintained in DMEM/F-12 (HyClone; GE Healthcare Life Sciences) with 10% FBS at 37°C with 5% CO_2 in a CO_2 incubator. The 293 cell line, a vehicle for the production of adenoviral vaccines and recombinant proteins (19), was purchased from the Type

Correspondence to: Dr Yu-Nong Wu, Department of Oral and Maxillofacial Surgery, Affiliated Hospital of Stomatology, Nanjing Medical University, 136 Hanzhong Road, Nanjing, Jiangsu 210000, P.R. China
E-mail: yjj1401@163.com

Culture Collection of the Chinese Academy of Science and maintained in modified Eagle's medium (MEM; HyClone; GE Healthcare Life Sciences) supplemented with 10% FBS (HyClone; GE Healthcare Life Sciences).

The interfering RNA for MSI1 (sh-MSI1) and negative plasmid (sh-Ctrl) were purchased from General Biosystems Co., Ltd. To construct the vector containing coding sequences of MSI1, cDNA was reverse-transcribed from total RNA extracted form HSC-3 cells, amplified with PCR with MSI1 primers and then cloned into the pcDNA3.1 vector. Approximately $1x10^6$ cells/per well were seeded and grown overnight in 6-well plates. On the following day, Lipofectamine 2000 reagent (Thermo Fisher Scientific, Inc.). was used for transient transfection of the cells with 3.0 μg plasmids, including sh-Ctrl, sh-MSI1, MSI1 overexpression plasmids (MSI1) or negative empty pcDNA3.1 vector (pcDNA3.1). At 48 h post-transfection, the cells were harvested for western blotting, reverse transcription-quantitative pcr (RT-qPCR) analysis, flow cytometry or other experiments at the indicated times.

For *in vivo* experiments, a lentiviral vector carrying interfering RNA for MSI1, pLKD-U6-MSI1-shRNA or a negative control vector, pLKD-U6-shRNA, and corresponding viruses ($1x10^8$ pfu) were custom-constructed and prepared by OBiO Technology (Shanghai) Corp., Ltd.

Luciferase reporter assay. The plasmids containing firefly luciferase reporters and MSI1-silencing plasmids were co-transfected into 293 cells using Lipofectamine 2000 (Thermo Fisher Scientific, Inc.). The cells were then lysed at 48 h after transfection and examined using a dual-luciferase assay (Promega Corporation) according to the manufacturer's instructions. Luciferase activity was expressed as the ratio of firefly to *Renilla* luciferase activity.

CCK-8 assay and BrdU incorporation. Approximately 5,000 cells were plated in 96-well plates with 200 μl medium per well. The cells were then transfected as indicated with sh-MSI1 (MSI1 suppression plasmid), negative control vector (pcDNA 3.1 or sh-Ctrl) or MSI1 overexpression plasmid (MSI1) for 48 h, after which time 2 μl CCK-8 solution (Biosharp) was added to each well and the cells were incubated for a further 4 h. The absorbance at 450 nm was measured using a microplate reader (Thermo Fisher Scientific, Inc.).

To detect BrdU incorporation, the cells transfected with the indicated plasmids were washed thoroughly with medium and then cultured in fresh medium containing 10 μM BrdU (Sigma-Aldrich; Merck KGaA) for 1 h. The cells were then allowed to grow in BrdU-free medium for another 48 h, after which time they were harvested for detection. The harvested cells were washed with PBS, fixed in 70% ice-cold ethanol, resuspended in 2N HCl and incubated for 30 min at room temperature, followed by hybridization with a mouse monoclonal anti-BrdU antibody (cat. no. ab8152, dilution, 1:500, Abcam) overnight at 4°C. Finally, the cells were rinsed with PBS combined with Tween-20 and incubated with fluorescein isothiocyanate-conjugated rabbit anti-mouse immunoglobulin antibody (Jackson ImmunoResearch), followed by staining with 4',6-diamidino-2-phenylindole solution for 10 min prior to image capture.

RT-qPCR analysis. RNA was isolated from tissues and cell lines using TRIzol reagent (Invitrogen; Thermo Fisher Scientific, Inc.). First-strand cDNA was synthesized using a TIANScript RT kit (Tiangen Biotech). Subsequently, the MSI1 expression levels were measured using SYBR-Green™ PCR Master Mix (Invitrogen; Thermo Fisher Scientific, Inc.), with β-actin serving as an endogenous control. The data were analyzed using the $2^{-\Delta\Delta Cq}$ method (20). The primer sequences for the genes were as follows: MSI1: Forward, 5'-GATCCAGGG GTTTCGGCTTC-3' and reverse, 5'-GAAGGCCACCTTAGG GTCAA-3'; β-actin: Forward, 5'-GATGAGATTGGCATGGC TTT-3' and reverse, 5'-GTCACCTTCACCGTTCCAGT-3'.

Cell invasion and migration. Transwell 24-well filters (pore size, 8 μm; BD Biosciences) were precoated with Matrigel at 37°C for 30 min. The cells transfected with the indicated plasmids were starved in serum-free medium overnight, and then suspended in medium containing 2% FBS. Approximately 20,000 cells were added to the upper chamber of the filters, and medium containing 20% FBS was added to the lower chamber. After incubating for 24 h, the cells on the lower surface of the membrane were fixed with cold methanol and stained with 0.1% crystal violet solution. For the migration assay, the cells were plated on Transwell 24-well filters in plates without Matrigel, and the protocol was the same as that used in the invasion assays described above. Finally, the cells in at least five random microscopic fields were counted and photographed.

Western blotting. Cell lysates from patient tissues and transfected cells were prepared with radioimmunoprecipitation assay lysis buffer (Beyotime Institute of Biotechnology), and protein concentrations were quantified using a bicinchoninic acid assay kit (Biosharp). Using electrophoresis on 10% sodium dodecyl sulfate-polyacrylamide gel, a total of 30 μg protein was separated and transferred to a polyvinylidene difluoride membrane (EMD Millipore). The membrane was then probed with antibodies against rabbit monoclonal pS727-STAT3 (cat. no. ab32143, dilution, 1:8,000), rabbit monoclonal STAT3 (cat. no. ab32500, dilution, 1:1,000), rabbit monoclonal c-Myc (cat. no. ab32072, dilution, 1:1,000), rabbit monoclonal cyclin D1 (cat. no. ab134175, dilution, 1:25,000), rabbit monoclonal MSI1 (cat. no. ab52865, dilution, 1:1,000), rabbit monoclonal p21 (cat. no. ab109520, dilution, 1:5,000), rabbit monoclonal p27 (cat. no. ab32034, dilution, 1:5,000) or mouse monoclonal β-actin (cat. no. ab6276, dilution, 1:6,000) at 4°C overnight. All antibodies were purchased from Abcam Biotechnology. After washing with a mixture of Tris-buffered saline and Tween 20, the membranes were incubated with horseradish peroxidase-conjugated anti-mouse or anti-rabbit antibody (Santa Cruz Biotechnology, Inc.) for 2 h at room temperature. The results were visualized using an enhanced chemiluminescence detection system (Bio-Rad Laboratories, Inc.), and the density of each band was analyzed using ImageJ software (National Institutes of Health).

Flow cytometry. For cell cycle analysis, ~$2x10^6$ cells were harvested and fixed overnight with 70% ethanol at -20°C. After washing twice with PBS, the cells were suspended in clean PBS with 50 μg/ml propidium iodide and 10 μg/ml RNase A

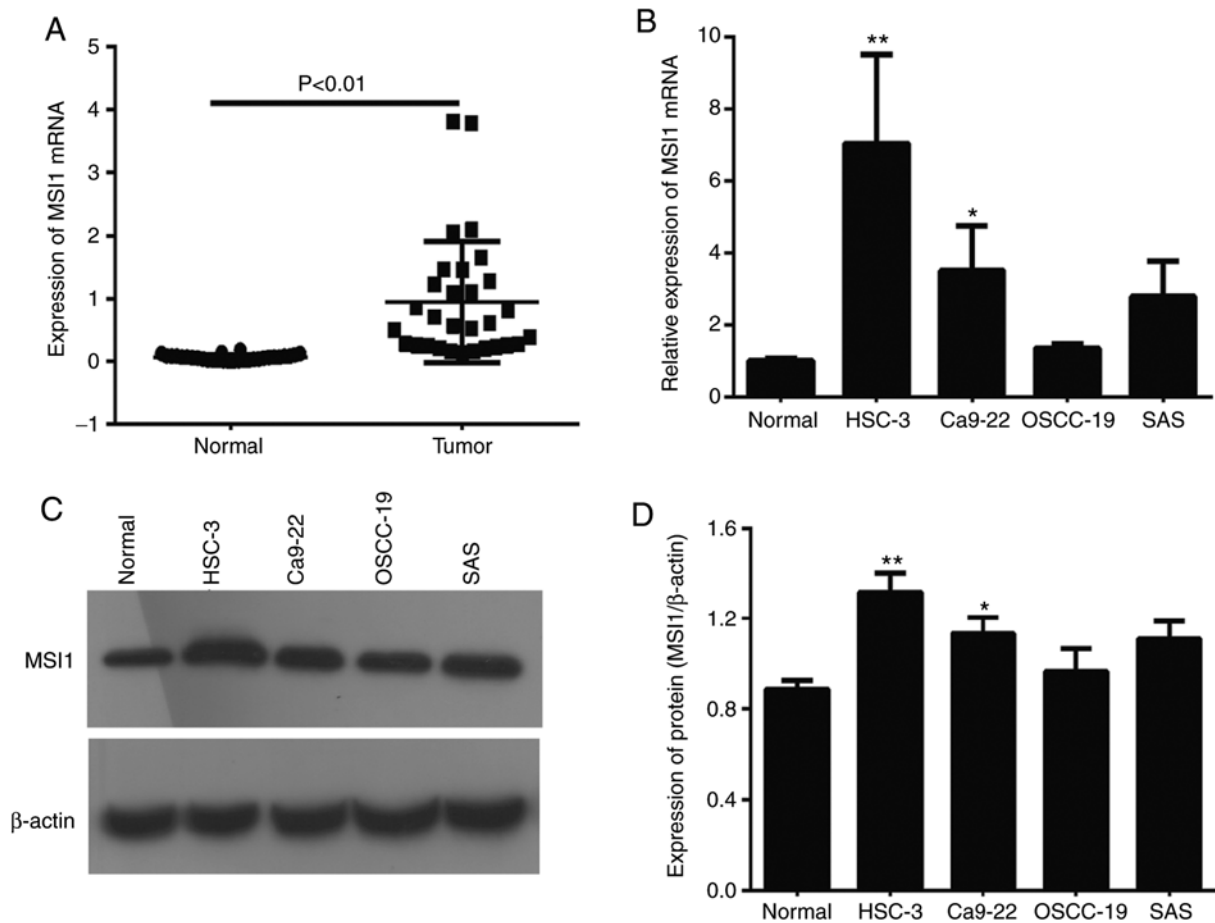Figure 1. MSI1 was upregulated in OSCC tissues and cell lines. (A) mRNA levels of MSI1 in OSCC tissues and adjacent healthy (normal) tissues. P<0.01 vs. normal. (B-D) mRNA and protein levels of MSI1 in OSCC cell lines; the results were normalized to the expression levels in normal tongue epithelial tissues. **P<0.05, **P<0.01 vs. normal. MSI1, Musashi RNA-binding protein 1; OSCC, oral squamous cell carcinoma.

for 30 min in the dark at room temperature. The cells were then analyzed using FACStar Flow Cytometry (BD Biosciences), and the cell cycle distribution was analyzed.

Tumor xenografts in nude mice. Five-week-old Balb/c female nude mice (Nu/Nu) were obtained from the Laboratory Animal Center of Nantong University. The animal experimental protocol was approved by the Institute of Animal Care and Use Committee of Nantong University (Nantong, China). Fresh surgical tumor tissues (F0) were collected immediately after surgery and cut into 2-3 mm^3-sized pieces in DMEM supplemented with penicillin-streptomycin. Tumor fragments were implanted into the right armpit of the mice. When the tumor size reached 100-200 mm^3, the samples (referred to as F1) were cut into pieces for passaging *in vivo* to create F2 xenograft tumors. When the F2 tumor size reached 100-200 mm^3, samples were collected and cut into 2-3-mm^3 pieces and implanted into the right armpit of mice to create F3. When the F3 tumor size had reached 10-20 mm^3, the mice were randomly divided into three groups (n=4 mice/group) and treated through the tail vein with different solutions as follows: The normal saline (NS) group received 100 μl saline solution; the negative control (NC) group received d pLKD-U6-shRNA lentivirus ($1x10^8$ pfu) in 100 μl saline; and the last group received pLKD-U6-MSI1-shRNA lentivirus ($1x10^8$ pfu) in 100 μl saline. Seven days later, lentivirus administration was

repeated. The tumor size and growth rate were monitored and measured using a caliper every 5 days. The approximate tumor volume (V) was calculated using the following equation: V=(longest diameter x shortest diameter^2)/2.

Statistical analysis. The results are shown as the mean ± standard deviation. The data were analyzed using the Duncan test following an analysis of variance for multiple comparisons. Differences were considered statistically significant when P<0.05.

Results

MSI1 is upregulated in OSCC tissues and cell lines. To determine MSI1 expression in OSCC, RT-qPCR analysis was conducted. The results demonstrated that the expression of MSI1 in OSCC tissues was markedly higher compared with that in adjacent healthy tissues (Fig. 1A). In addition, MSI1 expression in the OSCC cell lines was increased compared with that in normal tongue epithelial tissues, and was highest in HSC-3 followed by Ca9-22 cells. However, as Ca9-22 cells have been contaminated with the MSK-922 cell line, which is of head and neck SCC origin, HSC-3 cells for further experiments. (Fig. 1B-D). These data indicated that MSI1 may contribute to OSCC progression, but the underlying mechanism requires further investigation.
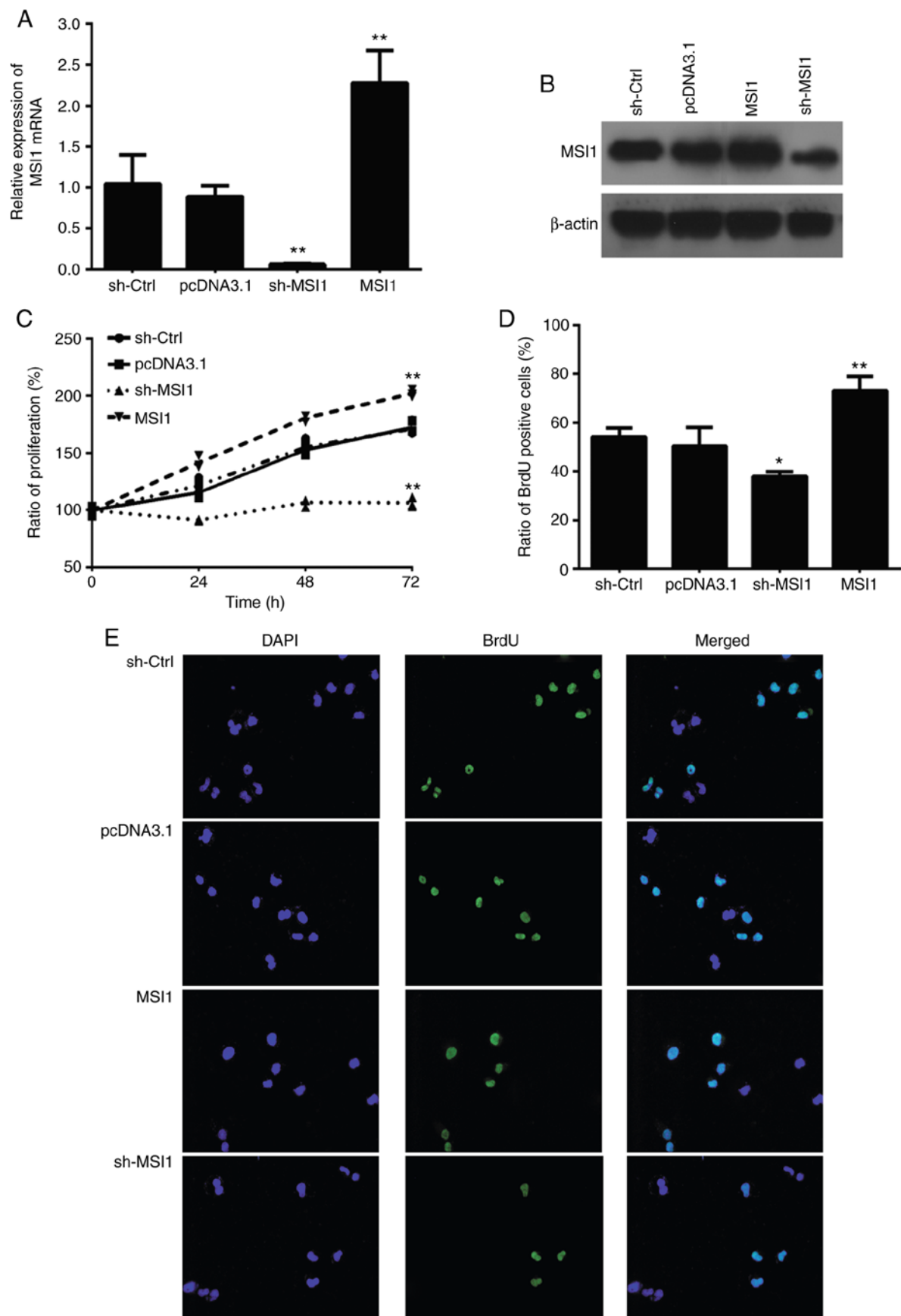
Figure 2. Knockdown of MSI1 inhibited proliferation of HSC-3 cells *in vitro*. (A and B) mRNA and protein levels of MSI1 in cells transfected with negative (sh-Ctrl) or MSI1 suppression plasmid (sh-MSI1), pcDNA3.1 empty plasmid, or MSI1 overexpression plasmid (MSI1), as determined by RT-qPCR and western blot assays, respectively. (C) CCK-8 assay for the proliferative ability of HSC-3 cells transfected with the indicated plasmids. (D and E) Immunofluorescence images of BrdU and DAPI in HSC-3 cells transfected with sh-MSI1, MSI1 overexpression plasmid or negative control. The ratio of BrdU-positive cells was analyzed with ImageJ software. $^*P<0.05$, $^{**}P<0.01$ vs. sh-Ctrl. MSI1, Musashi RNA-binding protein 1; RT-qPCR, reverse transcription-quantitative polymerase chain reaction.
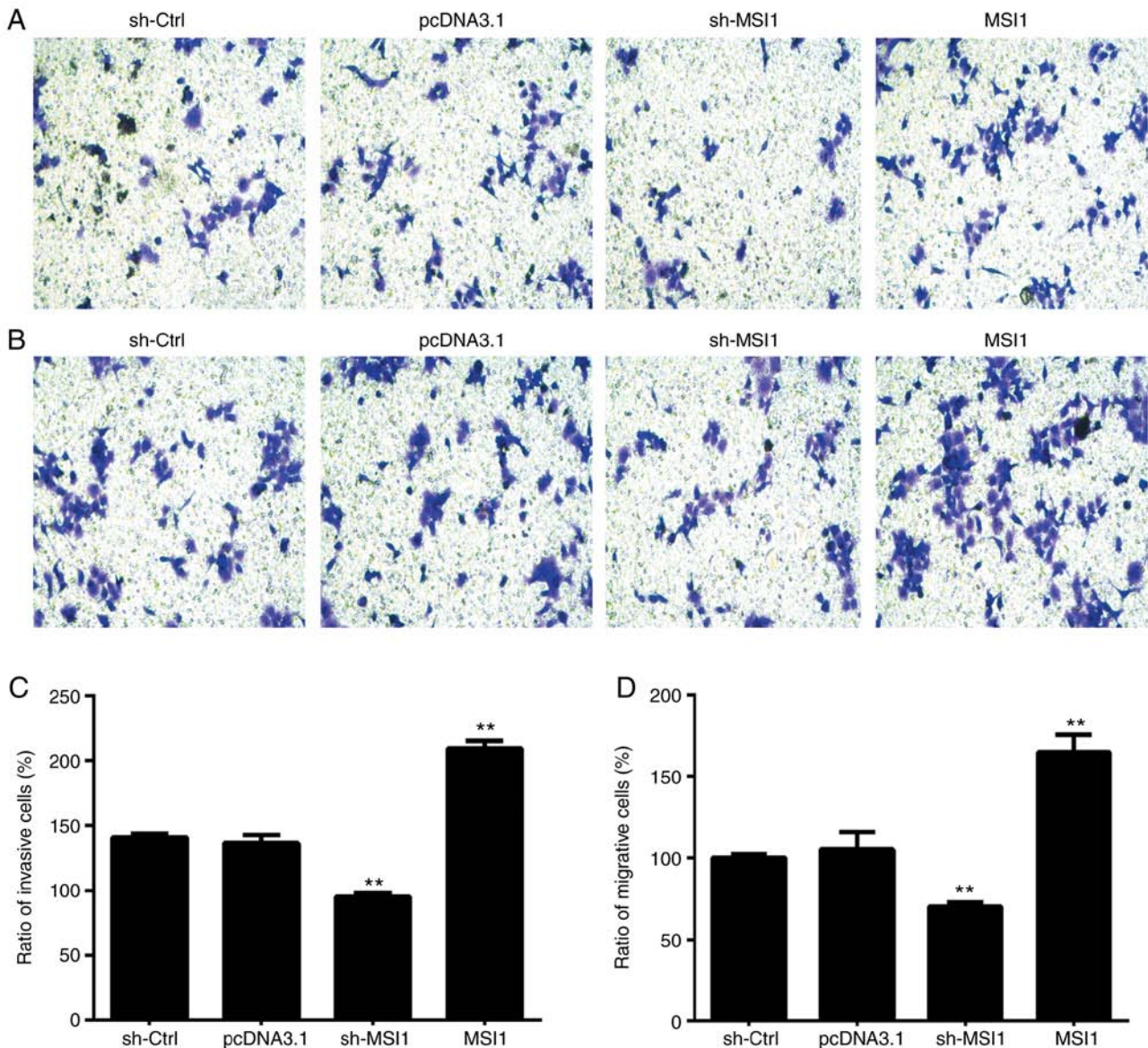
Figure 3. Knockdown of MSI1 inhibited the invasive and migrative capacity of OSCC cells *in vitro*. Representative images of the (A) invasion and (B) migration of cells transfected with the indicated plasmids (magnification, x200). The number of (C) invading and (D) migrating cells was counted in five random fields. **P<0.01 vs. sh-Ctrl. MSI1, Musashi RNA-binding protein 1; OSCC, oral squamous cell carcinoma.

Knockdown of MSI1 inhibits OSCC cell proliferation, invasion and migration in vitro. To assess the effect of MSI1 on the proliferation and apoptosis of OSCC cells, we established HSC-3 cells with either MSI1 suppression or MSI1 overexpression plasmids. MSI1 expression increased in the MSI1 group, but decreased in the sh-MSI1 group, at both the mRNA and protein levels in HSC cells (Fig. 2A and B). The CCK-8 assay then revealed that MSI1 silencing inhibited cell proliferation compared with control cells (Fig. 2C). In addition, the ratio of BrdU-positive cells among HSC-3 cells with MSI1 suppression was significantly increased compared with that in the control cells (Fig. 2D and E). The results also demonstrated that MSI1 suppression in OSCC cells resulted in markedly lower invasive and migratory ability compared with control cells (Fig. 3).

Knockdown of MSI1 inhibits the growth of OSCC cells in vivo. To further investigate the effect of MSI1 on tumor formation,

human OSCC tissues were transplanted into nude mice. The mice were then injected through the tail vein with saline solution (NS), negative control (NC) or MSI1 suppression viral vector. The increase in tumor volume was measured every 5 days. As shown in Fig. 4, MSI1 silencing inhibited tumor growth compared with that in the NS and NC groups. In addition, tumor weight was lower in the sh-MSI1 group compared with that in the NS or NC groups. Western blot analysis revealed that the levels of MSI1 significantly decreased following injection with the sh-MSI1 virus. These data indicate that MSI1 knockdown inhibited the tumor-forming ability of OSCC cells *in vivo*.

Knockdown of MSI1 results in OSCC cell cycle arrest by targeting c-Myc. Cell proliferation is directly associated with modulation of the cell cycle; therefore, the cell cycle distribution was then analyzed using flow cytometry. As shown in Fig. 5A and B, the proportion of HSC-3 cells with MSI1
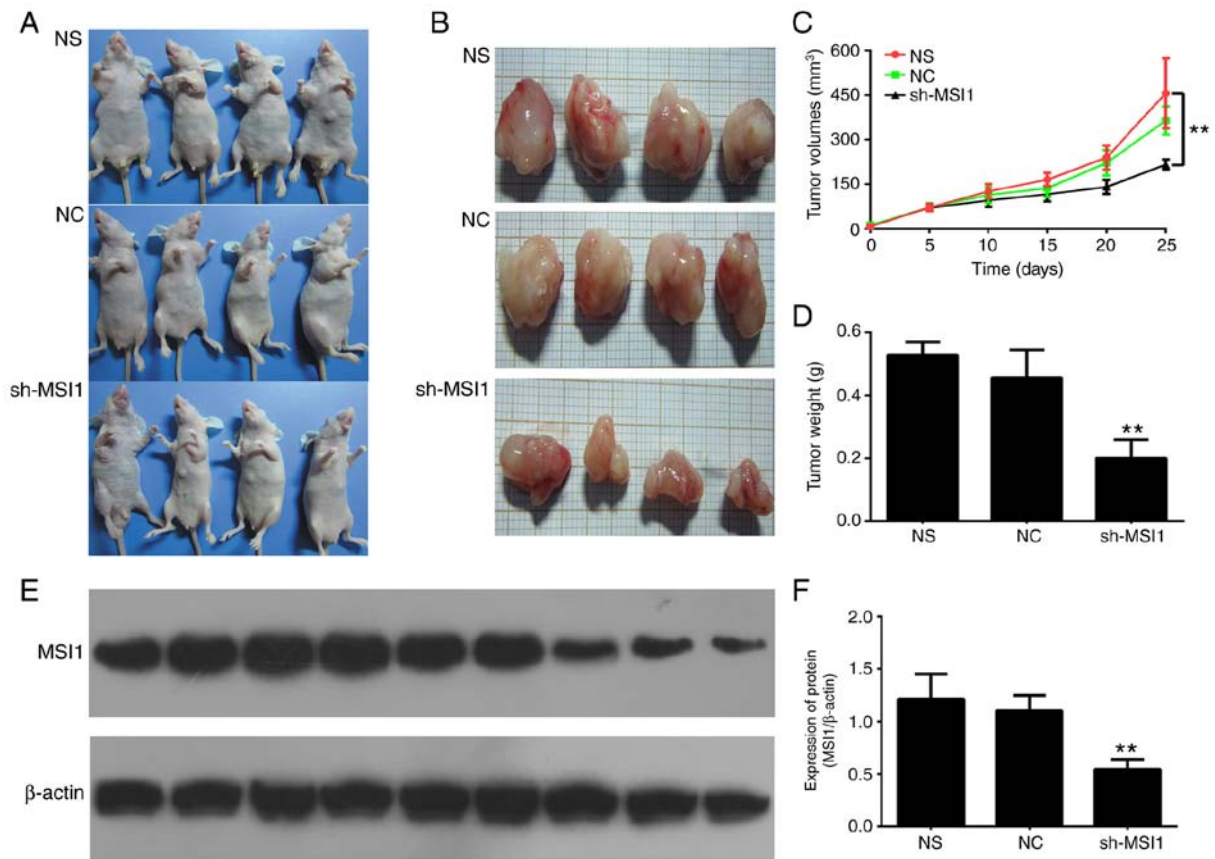
Figure 4. MSI1 suppression inhibited the growth of OSCC xenografts *in vivo*. (A and B) Representative images of patient OSCC tissue-derived xenografts. NS indicates xenografts injected through the tail vein with saline solution; NC indicates xenografts injected with negative control virus; sh-MSI1 xenografts were injected with MSI1 suppression plasmid. (C) Curves of tumor growth in xenografts receiving different treatment. (D) Tumor weight of xenografts receiving different treatment. (E and F) Representative images and density analyses of the expression of MSI1 in xenografts receiving different treatment, as determined by western blot analysis. Each lane group indicates independent tumor tissues; Lanes 1-3, NS; lanes 4-6, NC; and lanes 7-9, sh-MSI1. **P<0.01 vs. NS. MSI1, Musashi RNA-binding protein 1; OSCC, oral squamous cell carcinoma.
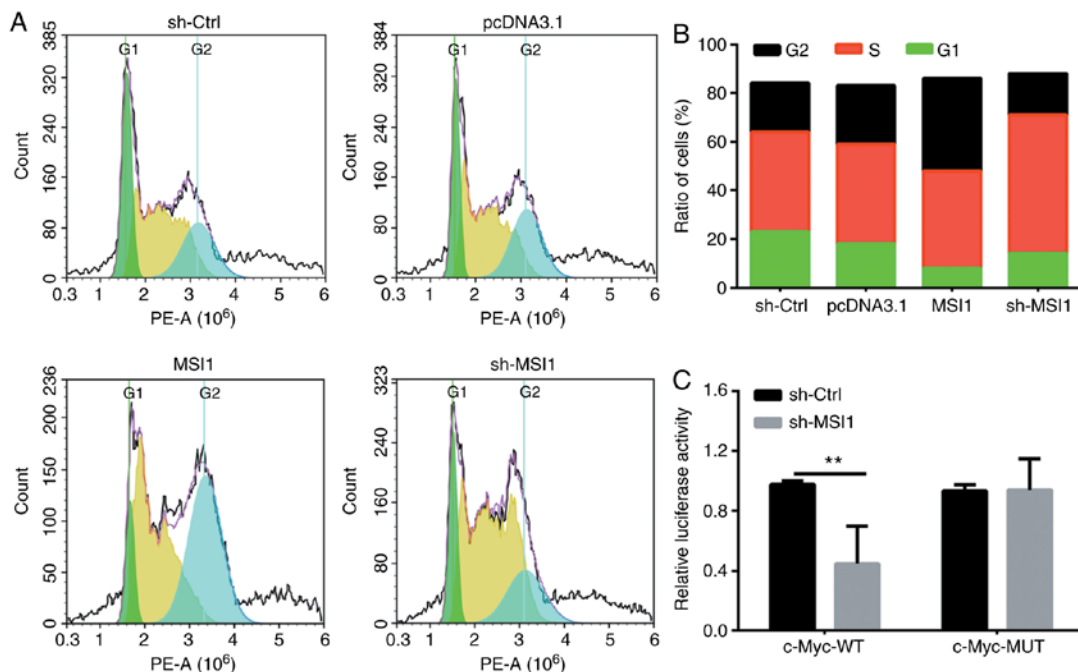

Figure 5. MSI1 suppression resulted in the cell cycle arrest of OSCC cells through binding to c-Myc. (A and B) Analysis of cell cycle for HSC-3 cells transfected with negative control plasmid (pcDNA3.1, sh-Ctrl), MSI1 suppression plasmid (sh-MSI1) or MSI1 overexpression plasmid (MSI1). (C) Relative luciferase activity assays of luciferase reporter plasmids containing c-Myc-wt or c-Myc-mut 3'-UTR performed in HSC-3 cells. **P<0.01 vs. sh-Ctrl group. MSI1, Musashi RNA-binding protein 1; OSCC, oral squamous cell carcinoma; UTR, untranslated region.
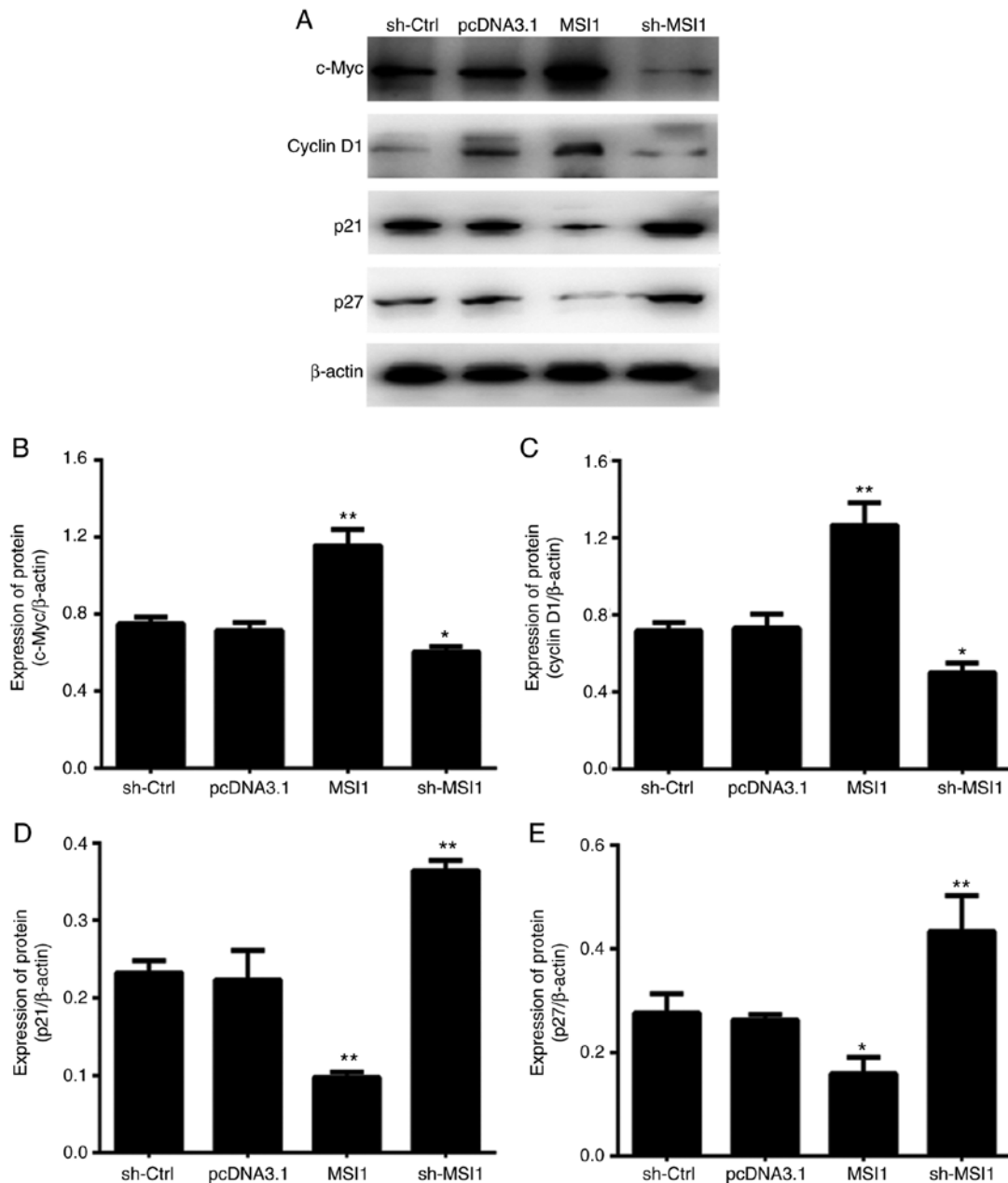
Figure 6. MSI1 suppression inhibited the activation of the cell cycle by binding to c-Myc. (A) Representative images of the expression of c-Myc, cyclin D1, p21 and p27 in HSC-3 cells transfected with the indicated plasmids. (B-E) Density analyses of the expression of c-Myc, cyclin D1, p21 and p27 in Ca9-22 cells transfected with the indicated plasmids. *P<0.05, **P<0.01 vs. sh-Ctrl. MSI1, Musashi RNA-binding protein 1.

suppression in the S phase was markedly higher compared with control cells.

To explore the molecular mechanism by which MSI1 regulates the OSCC cell cycle, the expression levels of c-Myc, cyclin D1, p21 and p27 were determined. Western blot analysis revealed that the expression of both c-Myc and cyclin D1 decreased in cells with MSI1 suppression; therefore, it was hypothesized that MSI1 may cause cell cycle arrest in part by inhibiting the expression of the c-Myc and cyclin D1 proteins (Fig. 6).

In addition, western blot analysis revealed that the expression of p21 and p27 was upregulated in OSCC cells exhibiting MSI1 suppression, which is consistent with previously reported results (21,22). Furthermore, predictive software (e.g., STRING, StarBase) indicated that c-Myc is also a target

downstream protein of MSI1, therefore, luciferase vectors containing wild-type and mutant MSI1-binding sequences were next constructed. The results revealed that the relative luciferase activity in cells with MSI1 suppression was significantly increased compared with that in the controls (Fig. 5C); however, no significant difference was observed between the MSI1 suppression and control groups in cells transfected by c-Myc mutant suppression vector. These results indicated that MSI1 suppression promoted cell cycle arrest, in part by binding to c-Myc.

Knockdown of MSI1 inhibits the activation of the STAT3 signaling pathway. A large body of evidence has shown that STAT3 expression plays a key role in cancer cell survival, growth and invasion. As shown in Fig. 7, activation of STAT3 at
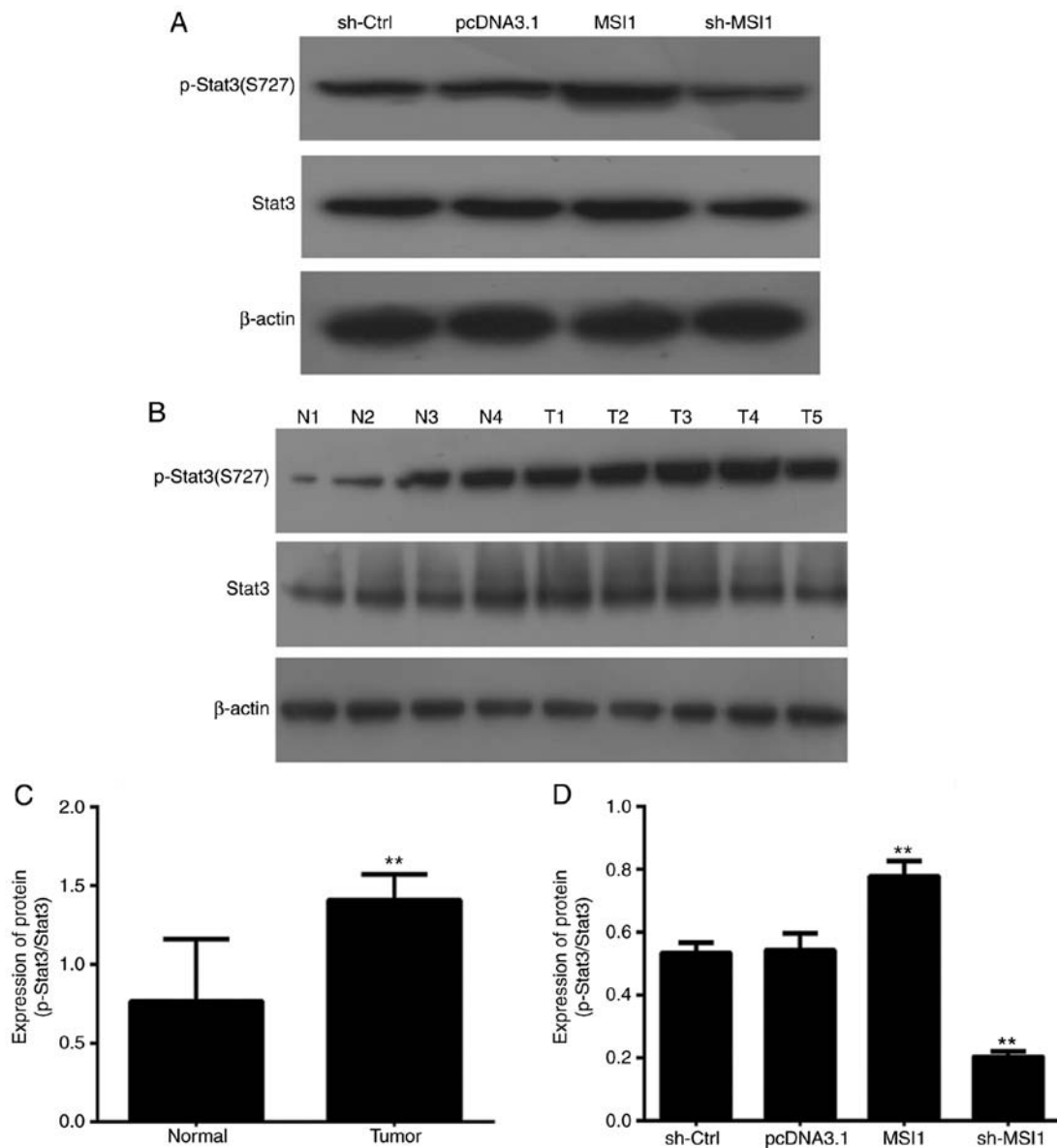
Figure 7. MSI1 suppression inhibited the activation of STAT3 signaling pathway. (A and D) Levels of p-S727-STAT3 and STAT3 in HSC-3 cells transfected with the indicated plasmids. **P<0.01 vs. sh-Ctrl. (B and C) Levels of p-S727-STAT3 and STAT3 in OSCC tissues and adjacent healthy tissues. T, tumor; N represents the adjacent normal tissues. **P<0.01 vs. adjacent healthy tissues. MSI1, Musashi RNA-binding protein 1; OSCC, oral squamous cell carcinoma; STAT3, signal transducer and activator of transcription 3.

Ser-727 was increased in OSCC tissues compared with that in adjacent healthy tissues, whereas STAT3 at Ser-727 was inhibited in HSC-3 cells following transfection with MSI1-silencing plasmids. These results indicated that MSI1 suppressed OSCC growth in part by inhibiting the activation of STAT3 signaling.

Discussion

Previous studies have proven that RNA-binding proteins are crucial for cell proliferation and apoptosis during the process of tumorigenesis (23-25). As a member of the MSI family of RNA-binding proteins, MSI1 was found to be overexpressed in several types of cancer, including non-small-cell lung cancer (14), osteosarcoma (21), and esophageal SCC (17).

In the present study, that the expression of MSI1 was found to be significantly increased in OSCC tissues and cell lines, which suggested that MSI1 is likely implicated in

OSCC. To further determine the mechanism through which MSI1 regulates OSCC cell proliferation, invasion or cell cycle arrest, MSI1 was either silenced or overexpressed in OSCC cells (HSC-3). The results demonstrated that MSI1 suppression significantly inhibited the proliferation and invasive capacity of cells *in vitro*, and significantly suppressed tumor growth *in vivo*. These data indicated that MSI1 acts as an oncogene, promoting cell proliferation and tumor growth. In addition, the results of the cell cycle analysis demonstrated that MSI1 suppression induced cell cycle arrest, which is considered to be an important factor in regulating cancer progression. Our findings were in agreement with those of previous studies on other types of tumors (26,27).

Based on StarBase, STRING, and previous studies, proteins associated with cell cycle arrest (e.g., p21 and p27l) and cell apoptosis (c-Myc) were the target RNAs of MSI1, and it has been reported that both p21 and p27 were the downstream

regulators of MSI1 in osteosarcoma (21); however, no studies have focused on the regulating mechanisms connecting MSI1 and c-Myc. The present study demonstrated that the expression of c-Myc and cyclin D1 was downregulated in HSC-3 cells with MSI1 suppression compared with that in control cells. In addition, luciferase assay demonstrated that MSI1 was able to directly bind to the consensus sequence of c-Myc 3'-UTR in OSCC cells. As a type of oncogene, c-Myc phosphoprotein can interact with the pre-replicative complex at the S phase of the cell cycle, and c-Myc silencing can cause cell-cycle arrest at the S phase and promote apoptosis in cancer cells, as previously shown in gastric cancer and esophageal SCC (28,29). Thus, MSI1 appears to cause cell cycle arrest in part by inhibiting the expression of c-Myc.

STAT3 has been proven to be a master regulator of several cancer hallmarks and enablers (30), and its activity is increased in ~50% of all cancers (31). In the present study, we found that STAT3 activation at Ser-727 was inhibited in OSCC tissues compared with adjacent healthy tissues, which is in accordance with the results reported by Deepak *et al* (31), Gkouveris *et al* (32), and others. In addition, STAT3 at Ser-727 was inhibited in HSC-3 cells following transfection with MSI1-silencing plasmids, and MSI1 suppression significantly decreased the invasiveness of HSC-3 cells. Accordingly, it may be hypothesized that MSI1 inhibits the invasion of OSCC cells by downregulating p-STAT3. As previously reported, aberrant regulation of STAT3 in oral cancer tumorigenesis promotes malignant behavior by regulating cell cycle progression, invasion and resistance to standard therapies (33); however, whether MSI1 silencing can regulate the progression of OSCC cell resistance by inhibiting STAT3 activation signaling remains unclear. The role of the MSI1/STAT3 axis in OSCC chemoresistance requires elucidation in future studies. In addition, although patient-derived xenograft (PDX) models can retain the histological and genetic characteristics of their donor tumors, and have been shown to be the preferred preclinical tool in translational cancer research compared with other conventional models, there was a limitation in the number of mice used in the present study. We hope to improve the accuracy of the results of *in vivo* experiments in future studies.

In conclusion, the results of the present study revealed that MSI1 is highly expressed in OSCC tissues, and that MSI1 silencing inhibits cell proliferation and tumor formation by cell cycle arrest, involving activation of c-Myc. In addition, MSI1 suppression inhibited the activation of STAT3 signaling, which plays an important role in OSCC, including OSCC chemo- and radioresistance. These findings uncovered a potential target in the clinical treatment of OSCC, but the potential role of MSI1 in OSCC chemoresistance requires further investigation. Furthermore, PDX models generated from human tumor samples may retain the histological and genetic characteristics of their tumors, and are the preferred preclinical tool compared with conventional models (34); however, there was still a limitation regarding the number of mice in this study, and the results of *in vivo* experiments must be verified in future studies.

Availability of data and materials

All the datasets generated and analyzed during the present study are included in the published manuscript.

Authors' contributions

CFW and HCZ performed the experimental study and data collection. CFW, XMF and XMS analyzed and interpreted the data. CHW and HCZ wrote and reviewed the manuscript. XMF and YNW revised the manuscript and provided material support. YNW conceived and supervised the whole project. All the authors have read and approved the final version of this manuscript.

Ethics approval and consent to participate

The study protocol was approved by the Ethics Committee of the Affiliated Hospital of Nantong University (Nantong, China) and all the patients provided written informed consent for their tissues to be used for the purposes of this study. All animal experiments were approved by the Institute of Animal Care and Use Committee of Nantong University (Nantong, China).

Patient consent for publication

Not applicable.

Competing interests

The authors declare that they have no competing interests to disclose.

References

1. Brocklehurst PR, Baker SR and Speight PM: Oral cancer screening: What have we learnt and what is there still to achieve? Future Oncol 6: 299-304, 2010.
2. Siegel RL, Miller KD and Jemal A: Cancer statistics, 2017. CA Cancer J Clin 67: 7-30, 2017.
3. Kessler P, Grabenbauer G, Leher A, Bloch-Birkholz A, Vairaktaris E and Neukam FW: Neoadjuvant and adjuvant therapy in patients with oral squamous cell carcinoma long-term survival in a prospective, non-randomized study. Br J Oral Maxillofac Surg 46: 1-5, 2008.
4. Gupta S, Kong W, Peng Y, Miao Q and Mackillop WJ: Temporal trends in the incidence and survival of cancers of the upper aerodigestive tract in Ontario and the United States. Int J Cancer 125: 2159-2165, 2009.
5. Kapoor A and Kumar S: Cancer stem cell: A rogue responsible for tumor development and metastasis. Indian J Cancer 51: 282-289, 2014.
6. Wang Y, Jiang CQ and Fan LF: Correlation of Musashi-1, Lgr5, and pEGFR expressions in human small intestinal adenocarcinomas. Tumour Biol 36: 6075-6082, 2015.
7. Liu XF, Yang WT, Xu R, Liu JT and Zheng PS: Cervical cancer cells with positive Sox2 expression exhibit the properties of cancer stem cells. PLoS One 9: e87092, 2014.

8. Wu XS, Xi HQ and Chen L: Lgr5 is a potential marker of colorectal carcinoma stem cells that correlates with patient survival. World J Surg Oncol 10: 244, 2012.

9. Chen HY, Lin LT, Wang ML, Tsai KL, Huang PI, Yang YP, Lee YY, Chen YW, Lo WL, Lan YT, *et al*: Musashi-1 promotes chemoresistant granule formation by PKR/eIF2α signalling cascade in refractory glioblastoma. Biochim Biophys Acta Mol Basis Di 1864: 1850-1861, 2018.

10. Gong P, Wang Y, Gao Y, Gao M, Liu L, Qu P, Jin X and Gao Q: Msi1 promotes tumor progression by epithelial-to-mesenchymal transition in cervical cancer. Hum Pathol 65: 53-61, 2017.

11. Guan A, Wang H, Li X, Xie H, Wang R, Zhu Y and Li R: MiR-330-3p inhibits gastric cancer progression through targeting MSI1. Am J Transl Res 8: 4802-4811, 2016.

12. Liu L, Qiu F, Chen J, Wu D, Nong Q, Zhou Y and Lu J: Functional polymorphism in the MSI1 gene promoter confers a decreased risk of lung cancer in chinese by reducing MSI1 expression. Curr Genomics 19: 375-383, 2018.

13. Lang Y, Kong X, He C, Wang F, Liu B, Zhang S, Ning J, Zhu K and Xu S: Musashi1 promotes non-small cell lung carcinoma malignancy and chemoresistance via activating the Akt signaling pathway. Cell Physiol Biochem 44: 455-466, 2017.

14. Qin G, Lian J, Yue D, Chen X, Nan S, Qi Y, Li B, Cui G, Li X, Zhao S and Zhang Y: Musashi1, a potential prognostic marker in esophageal squamous cell carcinoma. Oncol Rep 38: 1724-1732, 2017.

15. Dahlrot RH: The prognostic value of clinical factors and cancer stem cell-related markers in gliomas. Dan Med J 61: B4944, 2014.

16. Moghbeli M, Forghanifard MM, Sadrizadeh A, Mozaffari HM, Golmakani E and Abbaszadegan MR: Role of Msi1 and MAML1 in regulation of notch signaling pathway in patients with esophageal squamous cell carcinoma. J Gastrointest Cancer 46: 365-369, 2015.

17. Pastò A, Serafin V, Pilotto G, Lago C, Bellio C, Trusolino L, Bertotti A, Hoey T, Plateroti M, Esposito G, *et al*: NOTCH3 signaling regulates MUSASHI-1 expression in metastatic colorectal cancer cells. Cancer Res 74: 2106-2118, 2014.

18. Livak KJ and Schmittgen TD: Analysis of relative gene expression data using real-time quantitative PCR and the 2(-Delta Delta C(T)) method. Methods 25: 402-408, 2001.

19. Niu J, Zhao X, Liu Q and Yang J: Knockdown of MSI1 inhibited the cell proliferation of human osteosarcoma cells by targeting p21 and p27. Oncol Lett 14: 5271-5278, 2017.

20. Jadhav S, Ajay AK, Trivedi P, Seematti J, Pellegrini K, Craciun F and Vaidya VS: RNA-binding protein Musashi Homologue 1 regulates kidney fibrosis by translational inhibition of p21 and Numb mRNA. J Biol Chem 291: 14085-14094, 2016.

21. Abdelmohsen K, Srikantan S, Kuwano Y and Gorospe M: miR-519 reduces cell proliferation by lowering RNA-binding protein HuR levels. Proc Natl Acad Sci USA 105: 20297-20302, 2008.

22. Busà R, Paronetto MP, Farini D, Pierantozzi E, Botti F, Angelini DF, Attisani F, Vespasiani G and Sette C: The RNA-binding protein Sam68 contributes to proliferation and survival of human prostate cancer cells. Oncogene 26: 4372-4382, 2007.

23. Sutherland LC, Rintala-Maki ND, White RD and Morin CD: RNA binding motif (RBM) proteins: A novel family of apoptosis modulators? J Cell Biochem 94: 5-24, 2005.

24. Shi C and Zhang Z: miR-761 inhibits tumor progression by targeting MSI1 in ovarian carcinoma. Tumour Biol 37: 5437-5443, 2016.

25. Akasaka Y, Saikawa Y, Fujita K, Kubota T, Ishikawa Y, Fujimoto A, Ishii T, Okano H and Kitajima M: Expression of a candidate marker for progenitor cells, Musashi-1, in the proliferative regions of human antrum and its decreased expression in intestinal metaplasia. Histopathology 47: 348-356, 2005.

26. Dominguez-Sola D, Ying CY, Grandori C, Ruggiero L, Chen B, Li M, Galloway DA, Gu W, Gautier J and Dalla-Favera R: Non-transcriptional control of DNA replication by c-Myc. Nature 448: 445-451, 2007.

27. Wang Y, Cheng J, Xie D, Ding X, Hou H, Chen X, Er P, Zhang F, Zhao L, Yuan Z, *et al*: NS1-binding protein radiosensitizes esophageal squamous cell carcinoma by transcriptionally suppressing c-Myc. Cancer Commun (Lond) 38: 33, 2018.

28. Mesquita FP, Pinto LC, Soares BM, de Sousa Portilho AJ, da Silva EL, de Farias Ramos IN, Khayat AS, Moreira-Nunes CA, Bezerra MM, de Lucas Chazin E, *et al*: Small benzothiazole molecule induces apoptosis and prevents metastasis through DNA interaction and c-MYC gene supression in diffuse-type gastric adenocarcinoma cell line. Chem Biol Interact 294: 118-127, 2018.

29. Hanahan D and Weinberg RA: Hallmarks of cancer: The next generation. Cell 144: 646-674, 2011.

30. Redell MS and Tweardy DJ: Targeting transcription factors for cancer therapy. Curr Pharm Des 11: 2873-2887, 2005.

31. Deepak Roshan VG, Sinto MS, Thomas S and Kannan S: Cyclin D1 overexpression associated with activation of STAT3 in oral carcinoma patients from South India. J Cancer Res Ther 14: 403-408, 2018.

32. Gkouveris I, Nikitakis N, Avgoustidis D, Karanikou M, Rassidakis G and Sklavounou A: ERK1/2, JNK and STAT3 activation and correlation with tumor differentiation in oral SCC. Histol Histopathol 32: 1065-1076, 2017.

33. Li R, You S, Hu Z, Chen ZG, Sica GL, Khuri FR, Curran WJ, Shin DM and Deng X: Inhibition of STAT3 by niclosamide synergizes with erlotinib against head and neck cancer. PLoS One 8: e74670, 2013.

34. Sun S and Zhang Z: Patient-derived xenograft platform of OSCC: A renewable human bio-bank for preclinical cancer research and a new co-clinical model for treatment optimization. Front Med 10: 104-110, 2016.